Journal of Solid State Chemistry 183 (2010) 776–783

Contents lists available at ScienceDirect

Journal of Solid State Chemistry

journal homepage: www.elsevier.com/locate/jssc

Structural study of the $NaCdVO_4$–$Cd_3V_2O_8$ and CdO–V_2O_5 sections of the ternary system Na_2O–CdO–V_2O_5

Hamdi Ben Yahia *, Etienne Gaudin, Cédric Feral-Martin, Jacques Darriet

ICMCB, CNRS, Université Bordeaux 1, 87 Avenue du Docteur Schweitzer, 33608 Pessac Cedex, France

ARTICLE INFO

Article history:
Received 7 October 2009
Received in revised form
18 January 2010
Accepted 20 January 2010
Available online 25 January 2010

Keywords:
Vanadate
Na_2CrO_4-type
Maricite
CdO–V_2O_5 system
Oxide materials
Crystal structure

ABSTRACT

The $NaCdVO_4$–$Cd_3V_2O_8$ and CdO–V_2O_5 sections of the ternary system Na_2O–CdO–V_2O_5 have been studied and the crystal structures of $Cd_3V_2O_8$ and $Cd_{18}V_8O_{38}$ compounds were determined from single-crystal X-ray diffraction data. $Cd_3V_2O_8$ crystallizes with the maricite-type structure in space group *Pnma*, a=9.8133(10) Å, b=6.9882(10) Å, c=5.3251(10) Å and Z=4, whereas $Cd_{18}V_8O_{38}$ crystallizes in space group *P*1 with a new-type structure, a=8.5761(14), b=8.607(3), c=12.896(2) Å, α=95.64(1), β=102.45(1), γ=108.42(1)° and Z=1. The $Cd_3V_2O_8$ structure is made up of $Cd1O_4$ infinite chains of edge-sharing $Cd1O_6$ octahedra which are parallel to the b direction. The $Cd1O_4$ chains are linked together by VO_4 tetrahedra and strongly distorted $Cd2O_4$ tetrahedra. The structure of $Cd_{18}V_8O_{38}$ is based on an ordered three-dimensional framework of cadmium and vanadium polyhedra that share corners. The distorted CdO_6 octahedra, CdO_5 trigonal bipyramids and CdO_5 square pyramids share corners, edges or faces.

1. Introduction

Two different structures are observed for Li*M*VO_4 compounds with *M* a transition metal. $LiMnVO_4$ [1] and $LiCdVO_4$ [2] crystallize with Na_2CrO_4-type structure, whereas $LiCoVO_4$ [3], $LiNiVO_4$ [4] and $LiCuVO_4$ [5] crystallize with spinel-type structure. The homologous phosphates Li*M*PO_4 (*M*=Mn, Fe, Co, Ni) [6–9] crystallize with the olivine-type structure. In $LiMnVO_4$, with Na_2CrO_4 structure, Manganese atoms are located in infinite chain of edge-shared octahedra. LiO_4 and VO_4 tetrahedra are sharing an edge; this leads to short distance between lithium and vanadium. This short distance between two cations induces strong steric strain in the structure and explains the weak occurrence of the Na_2CrO_4-type structures. In the case of phosphate compounds, synthesized at atmospheric pressure, only the $NaHgPO_4$ compound crystallizes with this structural type [10]. When P^{5+} replaces V^{5+} the P–O distances are shorter and then shortest metal–phosphorus distance is expected. In the case of $NaHgPO_4$ the sodium atoms are located in the infinite chain of edge-shared octahedra, the mercury atoms being located in the tetrahedral site instead of alkali cation. This tetrahedron share one edge with the PO_4 tetrahedron, the mercury position is significantly shifted away the shared edge close to the opposite edge to maximize the Hg–P distance. The steric strain in this Na_2CrO_4-type structure has been reduced because Hg^{2+} can be stabilized in linear coordination. This strong steric strain between cations in the edge-shared tetrahedra can be removed if one of these tetrahedra is empty. This is the case for the *M*PO_4 phosphates $FePO_4$-II, $TiPO_4$, VPO_4 and β-$CrPO_4$ which crystallize with the α-$CrVO_4$ structure-type [11–14]. The α-$CrVO_4$ structure corresponds to the Na_2CrO_4 structure where the sodium in the tetrahedral site is removed. Another way to overcome these steric strains is to applied pressure for the synthesis. Thus the $LiFePO_4$ and $LiNiPO_4$ compounds undergo transition from olivine-type to the Na_2CrO_4-type structure under a pressure of 65 kbar at 1173 K [15].

In a previous work it has been shown that in the system $LiCdVO_4$–$Li_{1/3}Cd_{1/3}\square_{1/3}CdVO_4$ the compounds crystallize with the Na_2CrO_4-type structure [2]. The Li^+ ions in the tetrahedral site are replaced by Cd^{2+} and vacancy to keep the charge safe. The replacement of lithium by the bigger cation Cd^{2+} increases the steric strain between vanadium and cadmium in the edge-shared tetrahedra. To accommodate this steric strain when the content of cadmium is $>20\%$ a modulation of the structure is observed. The replacement of lithium by cadmium was limited to one third of cadmium leading to the compound $Li_{1/3}Cd_{1/3}\square_{1/3}CdVO_4$ or $LiCd_4(VO_4)_3$ [16].

The aim of this work is to study the structural evolution of the $NaCdVO_4$–$Na_{1/3}Cd_{1/3}\square_{1/3}CdVO_4$ system. Previous works have shown that $NaCdVO_4$ crystallizes with the Na_2CrO_4-type structure [17,18] and $Na_{1/3}Cd_{1/3}\square_{1/3}CdVO_4$ ($NaCd_4(VO_4)_3$) [19] with the maricite structure. On contrary to the lithium-based homologous system, a high content of cadmium within the tetrahedral site of sodium induces structural change instead of the modulation of the Na_2CrO_4-type structure. In order to check if between the

* Corresponding author. Fax: +49 251 83 36002.
E-mail address: benyahia.hamdi@voila.fr (H.B. Yahia).

0022-4596/$ - see front matter © 2010 Elsevier Inc. All rights reserved.
doi:10.1016/j.jssc.2010.01.018

composition $NaCdVO_4$ and $Na_{1/3}Cd_{1/3}\square_{1/3}CdVO_4$ modulated structures are present the study of the $NaCdVO_4$–$Na_{1/3}Cd_{1/3}\square_{1/3}CdVO_4$ system has been started. As a different structure is observed for $Na_{1/3}Cd_{1/3}\square_{1/3}CdVO_4$ compared to $Li_{1/3}Cd_{1/3}\square_{1/3}CdVO_4$, the replacement of more sodium by cadmium has been also tested and it has been shown that it is possible to gradually replace all sodium by cadmium up to the $Cd_{1/2}\square_{1/2}CdVO_4$ ($Cd_3V_2O_8$) composition. In the first synthesis of this latter compound several phases have been observed in the sample. Only one X-ray powder study of the $Cd_3V_2O_8$ phase is reported in the literature [20] and the structure of this compound is unknown. The analysis of the corresponding JCPDS-card (no. 28-0203) shows that this powder pattern corresponds also to a mixing of several phases. To understand these results, the CdO–V_2O_5 system has been reinvestigated and we have been able to structurally characterize $Cd_3V_2O_8$ and to find the new compound $Cd_{18}V_8O_{38}$.

2. Experimental

2.1. Synthesis and crystallization

In the section $NaCdVO_4$–$Cd_3V_2O_8$ the compounds with general formula $Na_{1-x}Cd_{x/2}\square_{x/2}CdVO_4$ have been prepared via two different ways of synthesis. For composition $x=0$ and $2/3 \le x \le 1$ the compounds were prepared by direct solid state reaction of a stoichiometric amounts of the starting reagents Na_2CO_3, V_2O_5 and CdO. The mixtures were heated at 600 °C for 12 h in platinum crucible under oxygen atmosphere to avoid CdO volatilisation and the starting reagents melting. Then powders were heated at 800 °C for 36 h with intermediate grindings to insure a total reaction. For $0 < x < 2/3$, $Na_{1-x}Cd_{x/2}\square_{x/2}CdVO_4$ compounds were prepared from the stoichiometric mixtures of $NaCdVO_4$ ($x=0$) and $NaCd_4(VO_4)_3$ ($x=2/3$). The mixtures were heated at 800 °C for 36 h in platinum crucible under oxygen atmosphere with several intermediate grindings.

For the composition $x=1$, even after several heat treatment at 800 °C, it was impossible to obtain a pure powder of $Cd_3V_2O_8$. To prepare only this phase it was necessary to increase the temperature up to 900 °C during 2 h to obtain the liquid state and then to quench it in water. It was not possible to prepare pure powder of $Cd_{18}V_8O_{38}$ even by quenching the phase in liquid state.

The melting of sample powders with nominal composition $Cd_3V_2O_8$ and $Cd_4V_2O_9$ at 950 °C followed by slow cooling at 2 °C/h down to 700 °C and 10 °C/h to ambient temperature gives several single crystals. In the case of $Cd_3V_2O_8$ composition we have obtained two kind of crystals corresponding to the $Cd_2V_2O_7$ and $Cd_3V_2O_8$ phases and a third amorphous phase whereas in the case of $Cd_4V_2O_9$ composition we have obtained two different crystals corresponding to $Cd_3V_2O_8$ and the new phase $Cd_{18}V_8O_{38}$.

2.2. X-ray powder diffraction measurements

X-ray powder diffraction patterns were measured with a Philips Xpert diffractometer using Bragg–Brentano geometry with Cu$K\alpha_1$ and Cu$K\alpha_1-\alpha_2$ radiations for, respectively, the compositions $x=1$ and $0 \le x < 1$. The X-ray data were collected in the 2θ range from 10° to 120° with a step of 0.02°. The X-ray diffraction data were refined by a Le Bail Profile analysis [21] using the Jana2000 programme package [22]. The background was estimated by a Legendre polynom and the peak shapes were described by a pseudo-Voigt function varying five profile coefficients [23]. The refinement of peaks asymmetry was performed using four parameters [24].

2.3. Single crystal X-ray measurements

The single-crystals of $Cd_{1/2}\square_{1/2}CdVO_4$ and $Cd_{18}V_8O_{38}$ were glued on a glass fibre and mounted on an Enraf-Nonius KappaCCD using Mo$K\alpha$ radiation ($\lambda=0.7107$ Å). Several single-crystals were tested and their quality assessed on the basis of the size and the sharpness of the diffraction spots. Data were corrected for Lorentz and polarisation effects with the Eval-CCD package [25]. The observed reflections could be indexed with orthorhombic and triclinic cells of dimensions $a=9.8133(10)$, $b=6.9882$ (10) and $c=5.3251$ (10) Å for $Cd_{1/2}\square_{1/2}CdVO_4$ and $a=8.5761(14)$, $b=8.607(3)$, $c=12.896(2)$ Å, $\alpha=95.64(1)$, $\beta=102.45(1)$ and $\gamma=108.42(1)°$ for $Cd_{18}V_8O_{38}$. The *Pnma* (#62) and $Pna2_1$ (#33), were found to be the possible space groups for $Cd_{1/2}\square_{1/2}CdVO_4$ and, $P\bar{1}$ (#2) and *P*1 (#1) for $Cd_{18}V_8O_{38}$. Based on these informations, the structure refinements were done using Jana2000 programme package. The atomic positions were determined using direct method with Shelx97 [26] and successive difference Fourier synthesis with Jana2000. Gaussian absorption correction, based on the shape of the crystal determined via the video camera of the Kappa CCD, was applied. The crystal data for the compounds are given in Table 1. The resulting atomic positions and anisotropic displacement parameters (ADPs) are given, respectively, in Tables 2 and 3 for $Cd_{1/2}\square_{1/2}CdVO_4$ and Table 5 and Appendix for $Cd_{18}V_8O_{38}$. Further details on the structure refinement may be obtained from the Fachinformationszentrum Karlsruhe, D-76344 Eggenstein-

Table 1
Crystallographic data and structure refinements for $Cd_3V_2O_8$ and $Cd_{18}V_8O_{38}$.

Formula	$Cd_{1.5}\square_{1/2}VO_4$	$Cd_{18}V_8O_{38}$
Crystal color	Orange block	Light green block
Crystal size (mm)	$0.012 \times 0.022 \times 0.053$	$0.03 \times 0.057 \times 0.097$
M (g mol^{-1})	283.6	3038.8
Crystal system	orthorhombic	triclinic
Space group	*Pnma*	P1
Parameters	$a=9.8133(10)$ Å	$a=8.5761(14)$ Å
	$b=6.9882(10)$ Å	$b=8.607(3)$ Å
	$c=5.3251(10)$ Å	$c=12.896(2)$ Å
		$\alpha=95.64(1)°$
		$\beta=102.45(1)°$
		$\gamma=108.42(1)°$
V (Å^3)	365.18(9)	867.7(4)
Z	4	1
Density calc., (g cm^{-3})	5.16	5.82
$F(000)$	508	1352
Temperature (K)		293(1)
Diffractometer		Enraf-Nonius KappaCCD
Monochromator		Oriented graphite
Radiation		Mo$K\alpha$ ($\lambda=0.71069$ Å)
Scan mode		CCD scan
$h\,k\,l$ range	± 15, ± 11, ± 8	± 13, ± 13, ± 20
θ_{min}, θ_{max}	4.15°, 36.67°	1.64°, 35°
Linear absorption coeff., (mm^{-1})	11.063	12.917
Absorption correction	Gaussian	Gaussian
T_{min}/T_{max}	0.671/0.880	0.345/0.686
R_{int}	0.1027	0.0834
No. of independent reflections	916	15 020
Reflections used [$I > 3\sigma(I)$]	436	12 993
No. of reflections	10 119	43 170
Refinement	F^2	F^2
No. of refined parameters	40	576
R factors $R(F)/wR(F^2)$	0.0277/0.0580	0.03756/0.0778
g.o.f.	1.04	1.27
x (Flack)		0.30(3)
Weighting scheme		$w=1/(\sigma^2(I)+0.0009I^2)$
Diff. Fourier residues (e$^-$ Å^{-3})	[−1.35, +1.02]	[−1.69, +1.42]

Table 2
Atomic positions and equivalent isotopic displacement parameters for $Cd_3V_2O_8$ (space group *Pnma*).

Atoms	Wyckoff position	Occupancy	*x*	*y*	*z*	U_{eq} (Å^2)
Cd1	4*a*	1	0	0	0	0.01853(12)
Cd2	4*c*	0.5	0.64660(10)	3/4	0.00460(19)	0.0254(3)
V	4*c*	1	0.18166(9)	1/4	0.4935(2)	0.0109(2)
O1	4*c*	1	0.1323(4)	1/4	0.8066(7)	0.0188(13)
O2	8*d*	1	0.6181(3)	0.0551(5)	0.1486(6)	0.0263(11)
O3	4*c*	1	0.8598(4)	1/4	0.0566(9)	0.0241(14)

Table 3
Anisotropic displacement parameters (Å^2) for $Cd_3V_2O_8$.

Atoms	U_{11}	U_{22}	U_{33}	U_{12}	U_{13}	U_{23}
Cd1	0.0172(2)	0.01293(18)	0.0254(3)	0.00435(13)	−0.0092(3)	−0.0059(2)
Cd2	0.0279(5)	0.0272(5)	0.0212(5)	0	−0.0051(6)	0
V	0.0084(3)	0.0155(4)	0.0087(4)	0	−0.0009(5)	0
O1	0.025(2)	0.022(2)	0.009(2)	0	0.0076(18)	0
O2	0.028(2)	0.0322(17)	0.0187(19)	−0.0132(16)	0.0058(14)	0.0026(16)
O3	0.0084(17)	0.0164(19)	0.048(3)	0	0.0007(19)	0

The anisotropic displacement factor exponent takes the form: $-2\pi^2[(ha^*)^2U_{11}+\cdots+2hka^*b^*U_{12}]$.

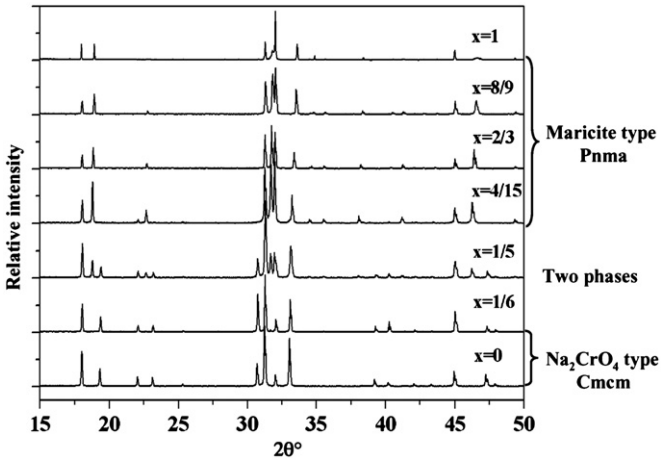

Fig. 1. X-ray powder patterns (Cu*K*α radiation) of the series of compounds $Na_{1-x}Cd_{x/2}\square_{x/2}CdVO_4$ with $0 \le x \le 1$.

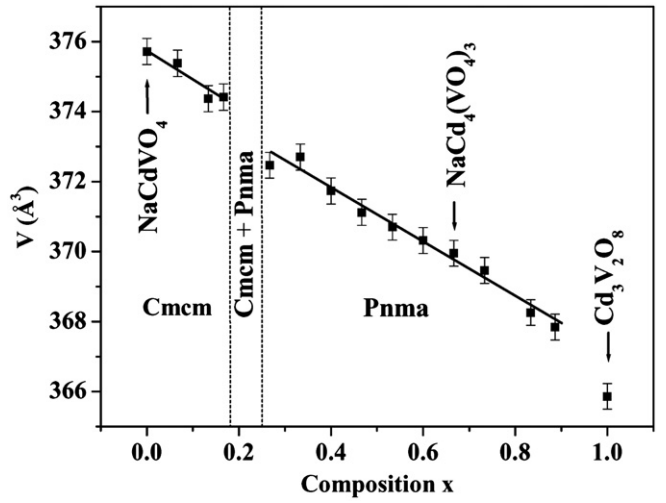

Fig. 2. Evolution of the cell volume with the composition *x* for $Na_{1-x}Cd_{x/2}\square_{x/2}CdVO_4$.

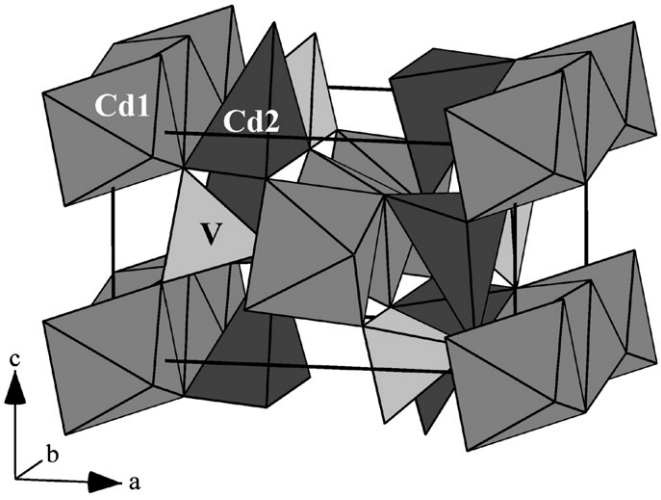

Fig. 3. Perspective view of $Cd_{1/2}\square_{1/2}CdVO_4$ structure.

Leopoldshafen (Germany), by quoting the Registry no. CSD–421348 and CSD–421347 for $Cd_3V_2O_8$ and $Cd_{18}V_8O_{38}$, respectively.

2.4. Single-crystal refinement

2.4.1. $Cd_3V_2O_8$

Extinction conditions observed for $Cd_3V_2O_8$ agree with the *Pnma* and $Pna2_1$ space groups. The structure of $Cd_3V_2O_8$ was solved and refined in the centrosymmetric *Pnma* space group, using the Jana2000 programme. The atomic positions were determined using direct method and successive difference-Fourier. With isotropic atomic displacement parameter (ADP), the residual factors converged to $R(F)=0.0838$ and $wR(F^2)=0.2125$ for 18 refined parameters. The use of anisotropic displacement parameter for all positions lowered them to $R(F)=0.0277$ and $wR(F^2)=0.0580$ for 40 refined parameters and 436 observed reflections with non-significant difference-Fourier residues (Table 1).

Table 4
Interatomic distances (Å) and bond valence sums (BVS, with coordination numbers in brackets) for $Cd_3V_2O_8$.

	Distance	BV
Cd1–O1(× 2)	2.408(3)	0.256
Cd1–O2(× 2)	2.235(3)	0.409
Cd1–O3(× 2)	2.244(3)	0.399
	⟨2.295⟩	BVS [6]=2.128
Cd2–O1	2.392(4)	0.267
Cd2–O2(× 2)	2.283(3)	0.359
Cd2–O2(× 2)	3.044(4)	0.046
Cd2–O3	2.386(5)	0.272
Cd2–O3	2.940(5)	0.061
	⟨2.336⟩	BVS [4]=1.257
	⟨2.625⟩	BVS [7]=1.41
V–O1	1.737(4)	1.195
V–O2(× 2)	1.678(3)	1.402
V–O3	1.768(4)	1.099
	⟨1.715⟩	BVS=5.098

Average distance values are given in brackets.$BV = e^{(r_0-r)/b}$ with the following parameters: b=0.37, r_0(Cd–O)=1.904 and r_0(V–O)=1.803 Å.

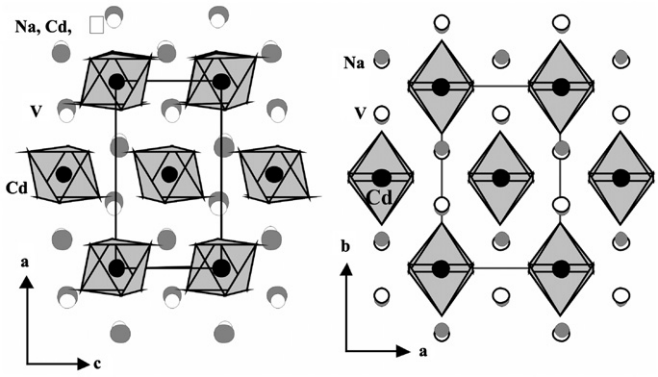

Fig. 4. On the left part, structure of $Na_{1/3}Cd_{1/3}\square_{1/3}CdVO_4$ (maricite-type) and on the right part, structure of $NaCdVO_4$ (Na_2CrO_4-type). White, black and grey circles represent V^{5+}, $Cd^{2+}$and Na^+ or Na^++Cd^{2+}atoms, respectively.

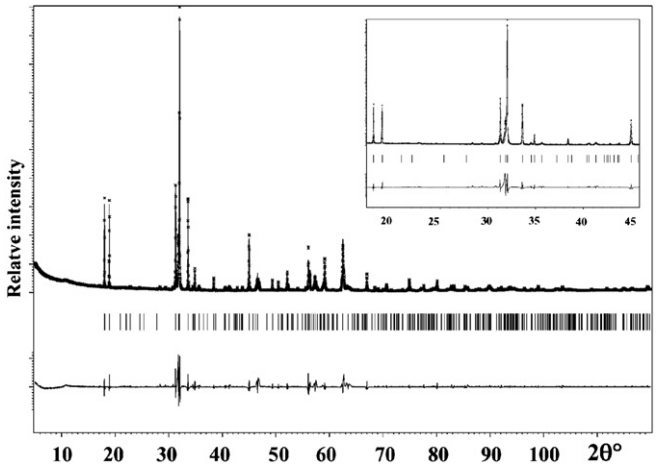

Fig. 5. Observed, calculated and difference plots for the XRPD (Cu$K\alpha_1$ radiation) profile refinement of the $Cd_{1/2}\square_{1/2}CdVO_4$ sample quenched in water at 900 °C.

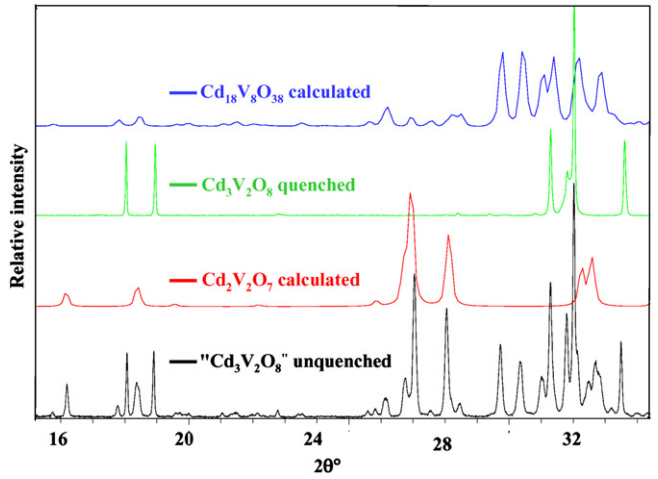

Fig. 6. Superposition of the XRPD of $Cd_2V_2O_7$ (calculated), $Cd_3V_2O_8$ (quenched) and $Cd_{18}V_8O_{38}$ (calculated) enabling the identification of the different phases in the unquenched $Cd_3V_2O_8$ sample.

2.4.2. $Cd_{18}V_8O_{38}$

In the first step, the structure of $Cd_{18}V_8O_{38}$ was refined in the centrosymmetric $P\overline{1}$ space group. The atomic positions were determined using direct method and successive difference-Fourier map analysis. With isotropic atomic displacement parameter (ADP), the residual factors converged to $R(F)$=0.1714 and w$R(F^2)$=0.3972 with large U_{iso} component for Cd9, O15, O16, O17, O18 and O19 atoms which indicates disorder of these positions. By splitting these positions and using anisotropic displacement parameters for all non-splitted atoms the residual factors were slightly improved ($R(F)$=0.1189 and w$R(F^2)$=0.3036) but some atoms have large anisotropic displacement parameters. Attempts performed to solve the structure in centrosymmetric space group $P\overline{1}$ failed; the structure was actually solved and refined in non-centrosymmetric space group $P1$. The refinement of the new atomic positions leads to the residual factors of $R(F)$=0.0562 and w$R(F^2)$=0.1288 for 255 refined parameters and 12 993 observed reflections. In final step anisotropic displacement parameters were refined and the residual factors fell down to $R(F)$=0.0376 and w$R(F^2)$=0.0778 for 576 refined parameters, with non-significant difference-Fourier residues (Table 1).

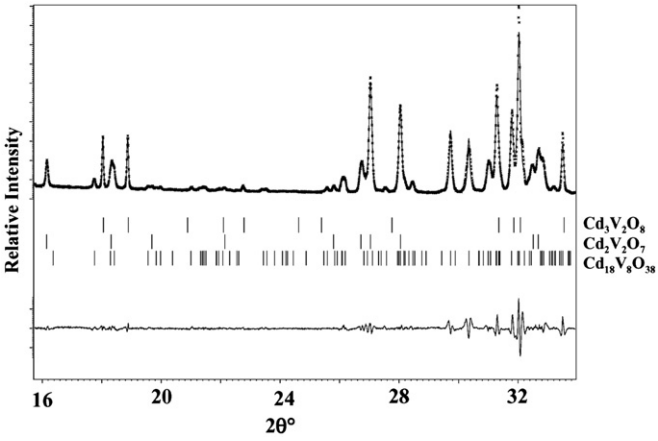

Fig. 7. Observed, calculated and difference plots for the XRPD (Cu$K\alpha_1$ radiation) profile refinement of the unquenched $Cd_{1/2}\square_{1/2}CdVO_4$ sample.

3. Results and discussion

3.1. $NaCdVO_4$–$Cd_{1/2}\square_{1/2}CdVO_4$ section

In the $(1-x)$ $NaCdVO_4$–x $Cd_{1/2}\square_{1/2}CdVO_4$ section two compounds have been previously studied: $NaCdVO_4$ (x=0) and $Na_{1/3}Cd_{1/3}\square_{1/3}CdVO_4$ (x=2/3). $NaCdVO_4$ crystallizes with Na_2CrO_4-type structure, whereas $Na_{1/3}Cd_{1/3}\square_{1/3}CdVO_4$ crystallizes with the maricite-type structure. Fig. 1 shows the evolution of the X-ray diffraction patterns of the $(1-x)$ $NaCdVO_4-x$ $Cd_{1.5}VO_4$ section for $x\in[0, 1]$. For $x\leq 1/6$ the compounds crystallize with the Na_2CrO_4 structure type. A structural change is clearly observed for $x>4/15$, the compounds crystallizing with the maricite type structure. The interval range $1/6 < x < 4/15$ corresponds to a zone of phase coexistence. This is in agreement with a previous work [27]. The evolution of the cell volume as a function of the composition is given in Fig. 2. The structural change is reflected by a discontinuity of this cell volume evolution between x=1/6 and 4/15. This evolution is linear for both zones. A different behaviour for $Cd_3V_2O_8$ is observed and may be attributed to the use of a different synthesis method (see experimental section). The decrease of the cell volume in all the x range is in good agreement with the replacement of Na^+ by smaller Cd^{2+} and vacancy, the Shannon radius of Na^+ and Cd^{2+} being equal to 1.02 and 0.95 Å (CN=6), respectively [28].

The decrease of the cell volume induces the increase of the steric strain in the $NaCdVO_4$ structure. Indeed, the b parameter decreases then the Cd^{2+}/Na^+–V^{5+}distance decreases (see discussion in Ref. [2] for instance (Li-system)). This increase of the repulsion between these cations induces the destabilization of the Na_2CrO_4-type structure. On contrary to the lithium based system $LiCdVO_4$–$Li_{1/3}Cd_{1/3}\square_{1/3}CdVO_4$, no modulation of the Na_2CrO_4-type structure has been observed when the alkali cations are replaced by cadmium and vacancy in the [0–1/6] x range. Instead of modulation to manage steric strains, when the content of cadmium is too high in the tetrahedral site, a structural change is observed. With this new structure a complete replacement of sodium by cadmium is now possible. Indeed, in the $Li_{1-x}Cd_{x/2}\square_{x/2}CdVO_4$ system the limit composition was $Li_{1/3}Cd_{1/3}\square_{1/3}CdVO_4$, whereas in the $Na_{1-x}Cd_{x/2}\square_{x/2}CdVO_4$ system the limit composition is $Cd_{1/2}\square_{1/2}CdVO_4$, i.e. $Cd_3V_2O_8$. The structural and compositional evolution in the system led us to predict the existence of the $Cd_3V_2O_8$ compound (x=1) with the maricite-type structure. Indeed, the first attempts to prepare a pure phase have failed and three different phases at least were observed. The existence of this compound was claimed by Brown [20] but from the analysis of the corresponding JCPDS card (no. 28-0203) it is clear that the synthesized compound was in fact a mixture of many phases. The only way we have found to prepare almost pure $Cd_3V_2O_8$ powder was to quench the phase in the liquid state. This

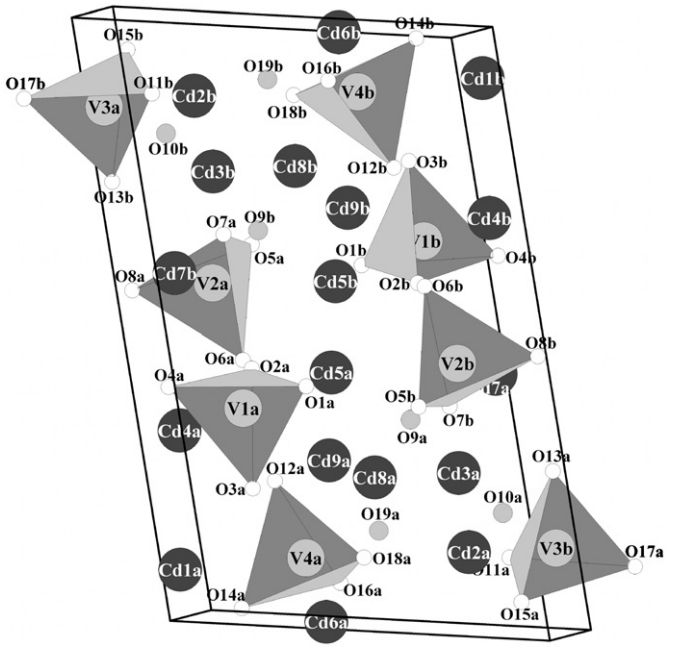

Fig. 8. Perspective view of $Cd_{18}V_8O_{38}$ structure.

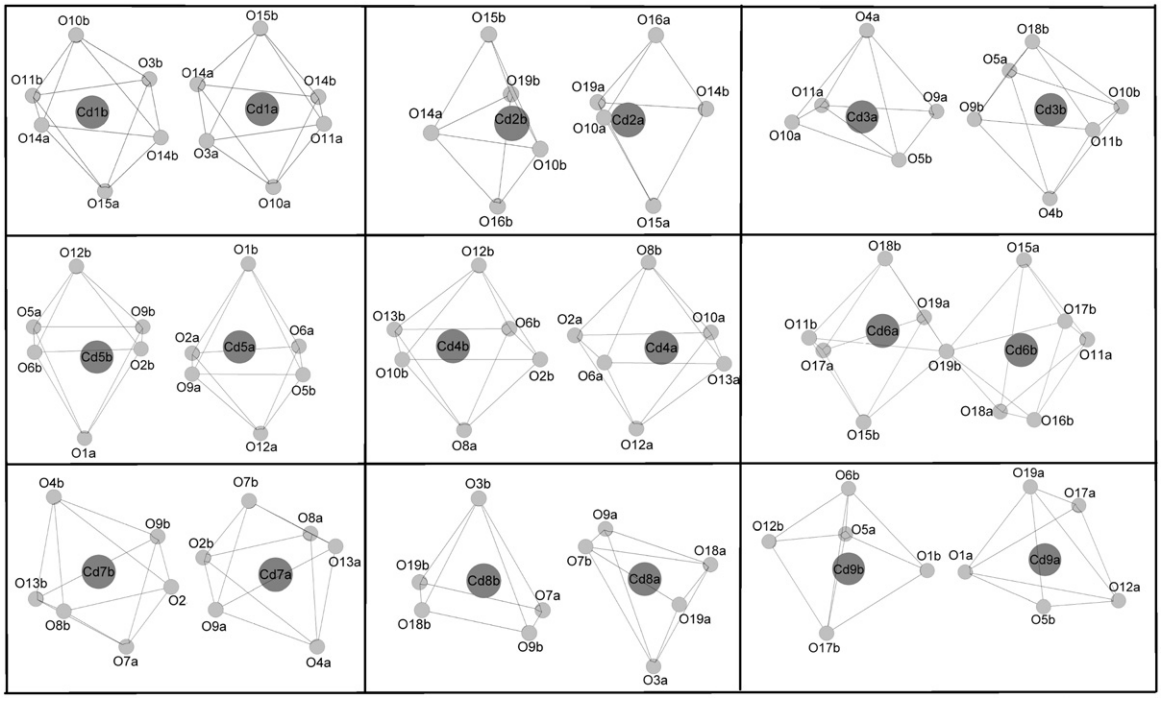

Fig. 9. CdO_n (n=5–6) polyhedra of $Cd_{18}V_8O_{38}$.

quenching needs to be very fast and often small impurities of $Cd_2V_2O_7$ are observed in the synthesised powders. When crystallization of $Cd_3V_2O_8$ is performed a mixing of many phases is always observed but single-crystals of the expected phase are also present in the preparation. It was then possible to refine the structure and to confirm that this structure derives from $Na_{1/3}Cd_{1/3}\square_{1/3}CdVO_4$ structure and more generally from the maricite-type structure.

The $Cd_3V_2O_8$ structure is made up of $Cd1O_4$ infinite chains of edge-sharing $Cd1O_6$ octahedra which are parallel to the *b* direction (Fig. 3). The $Cd1O_4$ chains are linked together by VO_4 tetrahedra and strongly distorted Cd_2O_4 tetrahedra. For the Cd1 position the average Cd1–O distance, 2.296 Å, is close to the sum of the shannon radii, 2.33 Å (Table 4). The V–O distances are ranging from 1.678 to 1.768 Å and are comparable to those observed in $Na_{1/3}Cd_{1/3}\square_{1/3}CdVO_4$. The bond valence sum for Cd1 and V, equal to 2.13 and 5.10, are close to the expected oxidation number +II and +V for cadmium and vanadium, respectively [29]. The coordination polyhedron of the Cd2 position is a strongly distorted tetrahedron with Cd–O distances ranging from 2.283(3) to 2.392(4) Å. The coordination polyhedron of Cd2 derives from the distorted NaO_6 octahedron observed in the mineral maricite, $NaFe_{0.9}Mn_{0.1}PO_4$ [30]. The bond valence sum calculated for the Cd2 position is equal to 1.09 by considering the 4 shortest Cd2–O distances. The coordination number of sodium in α-$NaCoPO_4$, with maricite structure, has been considered by Hammond et al. [31] equal to 10 for the BVS calculation. This coordination number is large and the Na ion is overbonded but if they consider a coordination number of 6, the sodium is still overbonded. The authors found a significant increase in the overbonding of sodium ion in the series Na*M*PO_4, *M*=Mn, Fe, Co, with an increase of the underbonding of the transition metal. They attributed the existence of a phase transition from the α form of $NaCoPO_4$ (maricite) to the β form (stuffed-tridimyte) to these two concomitant effects. In $Cd_3V_2O_8$ the Cd1 position which corresponds to the position of transition metal in maricite is slightly overbonded (BVS=2.13), whereas Cd2 in the sodium site is strongly underbonded with BVS=1.26. For this last position a bond–valence analysis is not pertinent because of the half-occupancy of the crystallographic site (Table 2). A relaxation of the polyhedra when cadmium is missing is expected.

The similarities between the powder pattern of the compounds with different structure in the system $(1-x)$ $NaCdVO_4$–x $Cd_{1/2}\square_{1/2}CdVO_4$ can be easily explained (see patterns for $x=0$ and 2/3 for instance, Fig. 1). Indeed in these two different structures, Na_2CrO_4- and maricite-type, the cation arrays are similar (Fig. 4). The oxygen arrays are different and this explains the difference in connection between the chains of edge-sharing octahedra and the difference of the other cations coordination polyhedra.

3.2. *CdO–V_2O_5 section*

The study of the $Na_{1-x}Cd_{x/2}\square_{x/2}CdVO_4$ system has enabled us to predict the existence of the $Cd_{1/2}\square_{1/2}CdVO_4$ compound ($x=1$) with the maricite-type structure. The synthesis of this composition at 900 °C followed by a quenching in water has led to almost a pure sample which was entirely indexed (Fig. 5), whereas the synthesis at 800 °C has led to a mixture of many phases. The analysis of the different crystals resulting from the crystallization of $Cd_3V_2O_8$ has allowed us to identify $Cd_2V_2O_7$ and $Cd_3V_2O_8$. Using the crystal data of these two phases, we have been able to index only a part of the powder pattern of the unquenched $Cd_3V_2O_8$ sample. Then, in order to identify the remaining non-indexed peaks, we have decided to reinvestigate the CdO richer composition $Cd_4V_2O_9$. There are significant divergences concerning the existence of this compound [32, and Refs. therein].

The different syntheses of the $Cd_4V_2O_9$ composition, performed at different temperatures, with or without quenching, have given the same XRPD pattern which is very similar to the unquenched $Cd_3V_2O_8$. Only the peaks corresponding to $Cd_2V_2O_7$ phase disappeared. By melting $Cd_4V_2O_9$ composition we have

Table 5
Atomic positions and equivalent isotopic displacement parameters for $Cd_{18}V_8O_{38}$.

Atoms	*x*	*y*	*z*	U_{eq} (Å^2)
Cd1*a*	0.2055	0.0259	0.0822	0.00991(14)
Cd1*b*	−0.20553(7)	−0.02495(8)	−0.08245(5)	0.01167(15)
Cd2*a*	0.86157(9)	0.72578(10)	0.12260(6)	0.01213(15)
Cd2*b*	−0.84709(9)	−0.72594(10)	−0.12338(6)	0.01193(15)
Cd3*a*	0.26780(10)	0.80070(10)	0.26723(6)	0.01351(16)
Cd3*b*	−0.26200(9)	−0.77586(10)	−0.26128(6)	0.01134(15)
Cd4*a*	0.04798(9)	0.10242(9)	0.31831(6)	0.00983(15)
Cd4*b*	−0.05317(9)	−0.08505(9)	−0.31908(6)	0.01030(15)
Cd5*a*	0.25417(10)	0.50743(10)	0.42395(6)	0.00995(15)
Cd5*b*	−0.26497(9)	−0.49705(10)	−0.43389(6)	0.00990(15)
Cd6*a*	0.59784(10)	0.34631(10)	−0.00109(6)	0.01315(16)
Cd6*b*	−0.62523(10)	−0.33925(10)	−0.00926(6)	0.01140(15)
Cd7*a*	0.64943(9)	0.89795(10)	0.42773(6)	0.01122(15)
Cd7*b*	−0.64866(9)	−0.87738(10)	−0.42605(6)	0.01194(15)
Cd8*a*	0.51904(10)	0.54726(11)	0.24652(7)	0.01771(19)
Cd8*b*	−0.50937(9)	−0.52690(10)	−0.23957(6)	0.01198(15)
Cd9*a*	0.83263(9)	0.39687(9)	0.26430(6)	0.01314(15)
Cd9*b*	−0.85387(9)	−0.36572(9)	−0.29701(6)	0.01266(15)
V1*a*	0.47402(16)	0.23225(17)	0.35200(10)	0.0080(3)
V1*b*	−0.46993(16)	−0.22128(17)	−0.35397(10)	0.0073(3)
V2*a*	0.00965(16)	0.25826(16)	0.56817(11)	0.0072(3)
V2*b*	−0.00623(17)	−0.23821(17)	−0.56551(11)	0.0072(3)
V3*a*	0.36988(17)	0.00516(18)	0.84535(10)	0.0072(3)
V3*b*	−0.37175(16)	−0.01481(18)	−0.85764(10)	0.0074(3)
V4*a*	0.08352(18)	0.37827(17)	0.11553(11)	0.0105(3)
V4*b*	−0.06431(16)	−0.37903(16)	−0.11971(10)	0.0072(3)
O1*a*	0.6745(7)	0.3865(8)	0.3895(5)	0.0154(17)
O1*b*	−0.6730(7)	−0.3741(8)	−0.3959(5)	0.0152(17)
O2*a*	0.3441(7)	0.2871(7)	0.4216(5)	0.0144(18)
O2*b*	−0.3412(7)	−0.2706(7)	−0.4280(4)	0.0115(16)
O3*a*	0.3969(7)	0.2318(8)	0.2204(4)	0.0148(17)
O3*b*	−0.3890(7)	−0.2358(7)	−0.2235(4)	0.0114(15)
O4*a*	0.4783(7)	0.0427(7)	0.3804(5)	0.0151(17)
O4*b*	−0.4716(7)	−0.0311(7)	−0.3723(5)	0.0145(18)
O5*a*	0.9327(7)	0.3879(7)	0.6380(4)	0.0101(15)
O5*b*	−0.9400(7)	−0.3674(7)	−0.6430(5)	0.0136(17)
O6*a*	0.0158(7)	0.3044(7)	0.4425(4)	0.0119(16)
O6*b*	−0.0124(7)	−0.2910(7)	−0.4404(4)	0.0131(17)
O7*a*	0.2052(7)	0.2861(8)	0.6462(5)	0.0183(18)
O7*b*	−0.2012(7)	−0.2555(7)	−0.6340(4)	0.0144(16)
O8*a*	0.8768(7)	0.0566(7)	0.5513(4)	0.0121(16)
O8*b*	−0.8715(7)	−0.0371(7)	−0.5496(4)	0.0143(17)
O9*a*	0.4236(6)	0.6779(6)	0.3487(4)	0.0087(15)
O9*b*	−0.4254(6)	−0.6627(7)	−0.3520(4)	0.0103(15)
O10*a*	0.0926(6)	0.9207(6)	0.2081(4)	0.0083(14)
O10*b*	−0.0901(6)	−0.9034(7)	−0.2053(4)	0.0103(15)
O11*a*	0.4098(6)	0.8828(7)	0.1270(4)	0.0107(15)
O11*b*	−0.4149(7)	−0.8866(7)	−0.1332(4)	0.0117(15)
O12*a*	0.0690(7)	0.3312(7)	0.2416(4)	0.0118(16)
O12*b*	−0.0773(7)	−0.3143(7)	−0.2426(4)	0.0135(17)
O13*a*	0.7476(7)	0.9968(8)	0.2679(5)	0.0166(18)
O13*b*	−0.7526(7)	−0.9919(8)	−0.2765(4)	0.0152(18)
O14*a*	0.0362(7)	0.1916(7)	0.0269(5)	0.0156(17)
O14*b*	−0.0277(7)	−0.2042(7)	−0.0256(4)	0.0102(15)
O15*a*	0.6820(6)	0.8638(6)	0.0475(4)	0.0117(15)
O15*b*	−0.6938(7)	−0.9005(7)	−0.0558(4)	0.0125(16)
O16*a*	0.9452(9)	0.4757(9)	0.0797(6)	0.029(3)
O16*b*	−0.9117(6)	−0.4699(7)	−0.1068(4)	0.0126(15)
O17*a*	0.6731(7)	0.1816(7)	0.1174(5)	0.0155(16)
O17*b*	−0.6654(7)	−0.1998(6)	−0.1477(4)	0.0118(15)
O18*a*	0.2809(8)	0.5107(9)	0.1169(5)	0.024(2)
O18*b*	−0.2534(6)	−0.5292(7)	−0.1266(4)	0.0143(16)
O19*a*	0.6812(6)	0.5161(6)	0.1546(4)	0.0129(15)
O19*b*	−0.5930(6)	−0.5535(6)	−0.0952(4)	0.0117(14)

Table 6
Interatomic distances (Å), angles (deg), coordination numbers and bond valence sums for $Cd_{18}V_8O_{38}$.

Atom *A*	d_{A-O} min (Å)	d_{A-O} max (Å)	$\langle d_{A-O}\rangle$ (Å)	$\langle O-A-O\rangle$ (deg)	C.N.	BVS
Cd1*a*	2.191	2.447	2.317		6	2.032
Cd1*b*	2.221	2.544	2.360		6	1.828
Cd2*a*	2.116	2.523	2.294		5	1.893
Cd2*b*	2.125	2.437	2.307		5	1.813
Cd3*a*	2.124	2.489	2.310		5	1.821
Cd3*b*	2.149	2.579	2.371		6	1.875
Cd4*a*	2.189	2.515	2.331		6	1.964
Cd4*b*	2.182	2.489	2.326		6	1.991
Cd5*a*	2.178	2.554	2.322		6	2.028
Cd5*b*	2.173	2.661	2.333		6	2.024
Cd6*a*	2.196	2.618	2.375		6	1.794
Cd6*b*	2.181	2.557	2.337		6	1.946
Cd7*a*	2.181	2.514	2.318		6	2.076
Cd7*b*	2.150	2.534	2.343		6	1.973
Cd8*a*	2.072	2.540	2.298		5	1.974
Cd8*b*	2.142	2.499	2.304		5	1.816
Cd9*a*	2.254	2.342	2.312		5	1.664
Cd9*b*	2.224	2.327	2.274		5	1.853
V1*a*	1.683	1.740	1.714	109.45	4	5.096
V1*b*	1.681	1.750	1.717	109.43	4	5.065
V2*a*	1.689	1.736	1.712	109.47	4	5.117
V2*b*	1.667	1.728	1.709	109.46	4	5.172
V3*a*	1.698	1.730	1.714	109.48	4	5.090
V3*b*	1.691	1.760	1.726	109.47	4	4.952
V4*a*	1.671	1.756	1.719	109.48	4	5.045
V4*b*	1.703	1.735	1.719	109.38	4	5.029

obtained two different crystals corresponding to $Cd_3V_2O_8$ and the new phase $Cd_{18}V_8O_{38}$ [$Cd_4V_2O_9$=1/3 $Cd_3V_2O_8$+1/6 $Cd_{18}V_8O_{38}$]. The theoretical XRPD pattern of $Cd_{18}V_8O_{38}$, calculated using the single crystal data, corresponds perfectly to the non-indexed peaks of the $Cd_3V_2O_8$ XRPD pattern (Fig. 6). The analysis of the XRPD profile (Fig. 7) has confirmed that the unquenched $Cd_3V_2O_8$ sample corresponding also to JCPDS no. 28-0203 file [20] is in fact a mixture of three phases $Cd_2V_2O_7$, $Cd_3V_2O_8$ and $Cd_{18}V_8O_{38}$ [$Cd_3V_2O_8$=$(1-x)$ $Cd_3V_2O_8$+3x/5 $Cd_2V_2O_7$+x/10 $Cd_{18}V_8O_{38}$]. The different attempts to synthesis a pure $Cd_{18}V_8O_{38}$ sample failed. Beside the main phase $Cd_{18}V_8O_{38}$ we obtained CdO as impurity. By quenching the phase in liquid state we obtained a glass.

The structure of $Cd_{18}V_8O_{38}$ is based on an ordered three-dimensional framework of cadmium and vanadium polyhedra that share corners. A projection view of the structure with drawing of the oxygen polyhedra around all the vanadium atoms is displayed in Fig. 8. The Cd^{2+} cations are bonded to either five or six oxygen atoms, resulting in a highly asymmetric coordination environments (Fig. 9). The distorted CdO_6 octahedra, CdO_5 trigonal bipyramids and CdO_5 square pyramids share corners, edges or faces.

The crystallographers and others will note that for space group *P*1 (no. 1) *Z*=1 is extremely rare and usually indicates higher (centrosymmetric) symmetry. Therefore, we have attempted to confirm the non-centrosymmetry by closely examining the structure. Using the PLATON suite of crystallographic programs [33], we have determined that expect Cd6*a*O_6 and Cd6*b*O_6 and Cd9*a*O_5 and Cd9*b*O_5 polyhedra, the vanadium and cadmium polyhedra form pairs which possess a centre of symmetry (Figs. 8 and 9). When one does not apply any shift to the centre of symmetry, the polyhedra around Cd3*a* and Cd3b would be not related by a centre of symmetry (Fig. 9).

The VO_4 tetrahedra are regular in shape with V^{5+}–O bonds ranging from 1.667 to 1.728 Å and average values ranging from 1.709 to 1.726 Å. This is slightly lower than the value of 1.735 Å estimated from the effective ionic radii of the four-coordinated $V^{5+}$and O^{2-} [28]. No significant deviation from the ideal tetrahedral angle of 109.5° is observed (Table 6). In the distorted cadmium polyhedra, the Cd^{2+}–O bonds ranging from 2.072 to 2.661 Å with average values ranging from 2.274 to 2.375 Å which are close to the sum of the shannon radii, 2.27 and 2.35 Å for five and six coordinated cadmium atoms, respectively [28]. The results of the bond valence sum (BVS) calculations [29] confirmed the expected charge balance $Cd^{II}_{18}V^{V}_{8}O^{-II}_{38}$; nevertheless few cadmium atoms are underbonded (Table 6). This could be due to a partial occupancy of these atomic positions; however, the refinement of all the cadmium occupancies did not show any significant divergence from the ideal composition.

4. Conclusions

The study of the $Na_{1-x}Cd_{x/2}\square_{x/2}CdVO_4$ system $0 \le x \le 1$ has demonstrated that the substitution of the sodium for the cadmium atoms induces a destabilisation of the Na_2CrO_4-type structure which transits to the Maricite-type structure. Due to this structural transition, the study of the compositions with $x > 2/3$ has been possible and has enabled us to predict the maricite structure of $Cd_{1/2}\square_{1/2}CdVO_4$ (x=1). The different analyses using powder and single crystal data have shown that the synthesis of $Cd_3V_2O_8$ is not trivial. The pure $Cd_3V_2O_8$ phase has been obtained only by quenching the phase in liquid state. By reinvestigation of the CdO–V_2O_5 system, we have been able to identify and solve the structures of two compounds $Cd_{1/2}\square_{1/2}CdVO_4$ and $Cd_{18}V_8O_{38}$. We have demonstrated that the $Cd_3V_2O_8$ phase corresponding to the JCPDS no. 28-0203 file is a mixture of three phases $Cd_2V_2O_7$, $Cd_{1/2}\square_{1/2}CdVO_4$ and $Cd_{18}V_8O_{38}$, whereas the $Cd_4V_2O_9$ phase is a mixture of two phases $Cd_{1/2}\square_{1/2}CdVO_4$ and $Cd_{18}V_8O_{38}$. The different attempts to synthesis a pure $Cd_{18}V_8O_{38}$ sample have failed, even by quenching the phase in liquid state. Beside the main phase $Cd_{18}V_8O_{38}$ we have obtained CdO as impurity.

Appendix. Supplementary materials

Supplementary materials associated with this article can be found in the online version at doi: 10.1016/j.jssc.2010.01.018.

References

[1] A.K. Pahdi, W.B. Archibald, K.S. Nanjundaswamy, J.B. Goodenough, J. Solid State Chem. 128 (1997) 267–272.
[2] E. Gaudin, H. Ben Yahia, F.J. Zuniga, J.M. Pérez-Mato, J. Darriet, Chem. Mater. 17 (9) (2005) 2436–2447.
[3] O.N. Leonidova, V.I. Voronin, I.A. Leonidov, R.F. Samigullina, B.V. Slobodin, Zh. Strukt. Khim. 44 (2003) 277–281.
[4] J.C. Bernier, P. Poix, A. Michel, Bull. Soc. Chim. Fr. (1963) 445–446.
[5] M.A. La Fontaine, M. Le Blanc, G. Ferey, Acta Crystallogr. C 45 (1989) 1205–1206.
[6] S. Geller, J.L. Durand, Acta Crystallogr. 13 (1960) 325–331.
[7] A.S. Andersson, B. Kalska, L. Haggstrom, J.O. Thomas, Solid State Ionics 130 (2000) 41–52.
[8] A. Pujana, J.L. Pizarro, A. Goni, T. Rojo, M.I. Arriortua, An. Quim. Int. 94 (1998) 383–387.
[9] S.A. Warda, S.-L. Lee, Z. Kristallogr. NCS 212 (1997) 319.
[10] M. Hata, F. Marumo, Acta Crystallogr. B 38 (1982) 239–241.
[11] N. Kinomura, M. Shimada, M. Koizumi, S. Kume, Mater. Res. Bull. 11 (1976) 457–460.
[12] R. Glaum, M. Reehuis, N. Stuesser, U. Kaiser, F. Reinauer, J. Solid State Chem. 126 (1996) 15–21.
[13] J.-P. Attfield, P.D. Battle, A.K. Cheetham, J. Solid State Chem. 57 (1985) 357–361.
[14] M.J. Isasi, R. Saez-Puche, M.L. Veiga, C. Pico, A. Jerez, Mater. Res. Bull. 23 (1988) 595–601.
[15] O. Garcia-Moreno, M. Alvarez-Vega, F. Garcia-Alvarado, J. Garcia-Jaca, J.M. Gallardo Amores, M.L. Sanjuan, U. Amador, Chem. Mater. 13 (2001) 1570–1576.

[16] E. Gaudin, H. Ben Yahia, M. Shikano, M. Ben Amara, H.C. zur Loye, J. Darriet, Z. Kristallogr. 219 (2004) 755–762.
[17] G. Le Flem, R. Olazcuaga, Bull. Soc. Chim. Fr. 7 (1968) 2769–2780.
[18] M. Azrour, L. El Ammari, Y. Le Fur, B. Elouadi, Ann. Chim. Sci. Mater. 29 (5) (2004) 95–104.
[19] S.C. Abrahams, P. Marsh, J. Ravez, Acta Crystallogr. C 39 (1983) 680–683.
[20] J.J. Brown, J. Am. Ceram. Soc. 55 (1972) 500–503.
[21] A. Le Bail, H. Duroy, J.L. Fourquet, Mater. Res. Bull. 23 (1988) 447–452.
[22] V. Petricek, M. Dusek, The crystallographic computing system Jana 2000, Institute of Physics, Praha, Czech Republic.
[23] P. Thompson, D.E. Cox, J.B. Hastings, J. Appl. Crystallogr. 20 (1987) 79–83.
[24] J.F. Berar, G. Baldinozzi, J. Appl. Crystallogr. 26 (1993) 128–129.
[25] A.J.M. Duisenberg, L.M.J. Kroon-Batenburg, A.M.M. Schreurs, J. Appl. Crystallogr. 36 (2003) 220–229.
[26] G.M. Sheldrick, SHELXS-97, Universität Göttingen, Göttingen, Germany, 1997.
[27] B.V. Slobodin, L.L. Surat, Russ. J. Inorg. Chem. 52 (10) (2007) 1620–1623.
[28] R.D. Shannon, Acta Crystallogr. A 32 (1976) 751–761.
[29] I.D. Brown, D. Altermatt, Acta Crystallogr. B 41 (1985) 244–247.
[30] P.B. Moore, Am. Mineral. 57 (1972) 1333–1344.
[31] R. Hammond, J. Barbier, Acta Crystallogr. B 52 (1996) 440–449.
[32] M. Bosacka, A. Blonska-Tabero, J. Therm. Anal. Cal. 93 (3) (2008) 811–815.
[33] A.L. Spek, PLATON, a multipurpose crystallographic tool, Utrecht University, Utrecht, The Netherlands, 2008.